INFORMATICS JOURNALS

Research Article

Journal of Natural Remedies
DOI: 10.18311/jnr/2026/54295

eISSN: 2320-3358 | Vol 26(4), 2026 | pp. 1065-1080

# QbD-driven Development and *In Vitro* Evaluation of an Ethosomal Gel Containing *Jatropha curcas* Seed Extract

**Mohammad Yosuf Malik Damani[1*] and Jagdish Kakadiya[2]**

[1]Faculty of Pharmacy, Parul Institute of Pharmacy and Research, Parul University, Waghodia, Vadodara - 391760, Gujarat, India; yusufdamani@gmail.com

[2]Department of Pharmacology, Parul Institute of Pharmacy and Research, Parul University, Waghodia, Vadodara - 391760, Gujarat, India

## Abstract

**Background:** Fungal skin infections are common and require improved therapies. *Jatropha curcas* contains bioactive antifungal phytoconstituents, but limited permeability restricts its use. Ethosomal gels enhance skin delivery, while computational modelling aids compound selection. Quality by Design (QbD) ensures optimised, reproducible formulation, offering an effective, plant-based approach for enhanced antifungal treatment. **Aim:** The present study explores an integrated approach combining phytochemical profiling, computational modelling, and Quality by Design (QbD) strategies to develop a *Jatropha curcas*-based ethosomal gel for enhanced antifungal therapy. **Methods:** Methanolic seed extracts of *Jatropha curcas* were subjected to phytochemical screening and GC-MS analysis, revealing a diverse five bioactive 9,12-Octadecadienoic Acid (Z, Z)-, N-Hexadecanoic Acid, 1,2,3,4- Tetrahydrobenzo[A]Fluorene, Z, Z-2,15-Octadecadien-1-Ol acetate, (Z)6, and (Z)9- Pentadecadien-1-Ol in order of % area. Key compounds identified were further evaluated through molecular docking against antifungal targets, followed by ADMET analysis to predict drug-likeness and pharmacokinetic properties. A Central Composite Design (CCD) was employed to optimise ethosomal formulation. **Results:** The optimised ethosomal formulation was incorporated into a topical gel and characterised using SEM and stability studies. The three best bioactive compounds in the extract have good binding affinity and stability with PDB ID: 6MA7, 9,12-Octadecadienoic acid (Z, Z)-, N-Hexadecanoic acid and (Z)6, (Z)9-Pentadecadien-1-Ol. Drug release kinetics revealed sustained release behaviour, with model Hixson Crowel or Higuchi model. Optimised ethosomal gel has 97 % drug release, and the extract showed 66%. *In vitro* antifungal studies demonstrated significant activity against *Candida albicans* in dose depended manner. *Microsporum canis* and *Microsporum audouinii* compared to the conventional extract gel. **Conclusion:** This study highlights the potential of *Jatropha curcas* ethosomal gel as a promising candidate for topical antifungal therapy, emphasising the utility of a multidisciplinary framework in herbal drug development.

**Major Findings:** *In silico* studies showed strong binding affinity of key compounds with antifungal target PDB ID: 6MA7 and acceptable ADMET properties. Significant dose-dependent antifungal activity was observed against *C. albicans*, *M. canis*, and *M. audouinii*. The study confirms the potential of *J. curcas* ethosomal gel as a promising topical antifungal therapy.

**Keywords:** Antimicrobial Study, CCD, Ethosomal Gel, GCMS, *In Silico*, Seed Extract

(Article Chronicle: Article Received on: 06.01.2026; Revised on: 12.03.2026; Accepted on: 01.04.2026)

## 1. Introduction

*Jatropha curcas (J. curcus)* belongs to the family *Euphorbiaceae*, which has long been utilised in conventional healthcare. Because of the wide variety of phytochemicals found in its many portions, this plant has attracted a lot of attention for its pharmacological qualities. Although it is poisonous, particularly in the seeds, meticulous extraction and processing have shown significant medicinal potential[1,2]. The extract

*Author for correspondence

from *J. curcus* showed the maximum effectiveness when tested over several organic extracts on *Salmonella typhimurium*, *Proteus vulgaris*, *Agrobacterium tumefaciens*, *E. coli*, and *Klebsiella pneumoniae*[1]. Seed kernels of defatted *J. curcus* had a high crude protein content (61.8%) and a low amount of acid detergent fibre (4.8%) and neutral detergent fibre (9.7%)[3]. The results of the content analysis showed that there is an uneven distribution of phorbol esters in the seeds, 4.22 ± 0.25-15.52 ± 0.06 mg/g in tegmens and 1.61 ± 0.07-5.00 ± 0.42 mg/g in endosperms, whereas testas and embryos had concentrations below 0.5 mg/g[4]. *J. curcus* L. has been marketed as an oilseed crop, specifically as a feedstock for the creation of biodiesel[5]; major toxic phorbol esters, phytate and trypsin inhibitor factors are reported in the seed[6]. The bioactive compound isovitexin in the leaves and 2-hexyl-decanoic acid and 2,4,6-trihydroxybenzoic acid in the stem bark latex are probably responsible for the antimicrobial actions[7]. Both Gram-positive and Gram-negative bacteria were significantly inhibited by the methanolic fraction of latex and cake, confirming the different classes of bioactive compounds; when compared to normal quercetin, reducing power showed a dose-dependent rise in concentration[8]. By analytical techniques like Thin-Layer Chromatography (TLC), Infrared Spectroscopy (IRS), and reversed-phase High-Performance Liquid Chromatography (HPLC), flavonoid content has been reported[9]. Aqueous extract may be utilised as an antibacterial agent to treat coliform-related illnesses[10]. This is a multipurpose plant and has the potential to be used for both medical purposes and the manufacture of biodiesel, used for the treatment of skin diseases, cancer, and digestive, respiratory, and infectious disorders[11]. The essential oil of leaf extract was used for its antibacterial activity against bacteria and yeasts, and these qualities could be used to treat microbial infections. 39 components were found in the oil according to the Gas Chromatography coupled with Mass Spectrometry (GCMS) examinatio[12]. Phytochemical, larvicidal, and antibacterial qualities of different parts of this plant cultivated in Mauritius have been studied[13]. Antifungal activity of ethanolic extract of flower and methanolic extract of root against *Aspergillus niger* and *Penicillium notatum* has been reported[14]. GC-MS analysis identified eleven distinct bioactive chemicals in the methanol stem extract and thirty-nine in the acetone root extract. Antibacterial, antioxidant, and phytochemical properties have been studied[15]. Leaf extracts of *Acacia nilotica* and *J. curcus* plants have antibacterial properties against strains of *Pseudomonas aeruginosa* and *Staphylococcus aureus* that are resilient to many drugs[16]. Against dental pathogens, antimicrobial properties have been demonstrated[17]. Polyphenolic contents of this plant have antioxidant potential, reported in aqueous, ethanol, and methanol stem bark extracts[18]. *J. curcus* and *J. gossypiifolia* have the potential to cure anti-hyperpigmenting, anti-neurodegenerative, antidiabetic, and antioxidant agents. According to HPLC-MS examination, the plants contain significant amounts of bioactive substances[19]. The goal of the current study is to assess the antifungal activity by optimising the ethosome gel formulation using QbD tools. Bioactive compounds in the extract have been identified through analytical techniques such as GCMS, and molecular docking and ADMET analysis have been used to predict the extract's pharmacological activity and safety. *In vitro* research has confirmed the antifungal activity. This study's scientific method is new; it aims to increase the drug's bioavailability and make it more affordable.

## 2. Materials and Methods

### 2.1 Materials

Sample collection and details: Test Organisms: *Candida alibicans* (MTCC, Chandigarh) MTCC No-7315, SDA agar (Cat No: M063, Himedia), Fluconazole Cat No: SD232, Himedia), DMSO (Fisher Scientific), double distilled water, sterile cotton swabs, sterile petriplates (Tarsons), laminar air flow (Alpha Linear), pipettes (10ul, 200ul and 1ml Pipettes) and Personal Protective Equipment (PPE), i.e., gloves, mouth mosque, head cap and lab coat etc. The microorganisms used for antimicrobial analysis were purchased from Microbial Type Culture Collection and Gene Bank (*MTCC*), Chandigarh. The fungal strain was maintained on SDA Agar (SDA). Test Organisms: *Microsporum canis* (MTCC, Chandigarh) MTCC No-2820, *Microsporum audouini* (MTCC, Chandigarh) ATCC 42558.

Collection of seeds: *J. curcas* plant species has been authenticated by Dr Haleshi C., Assistant Professor, Plant Taxonomy and Medicinal Plant Laboratory, Department of Studies in Botany, Davangere, Karnataka, India.

## 2.2 Methods

Methods of extraction: Five kg of seeds were gathered and thoroughly cleaned under running water. Then leave them outside for two weeks to dry. The dried seeds were ground into a powder using a mixer grinder before being run through filter number 22. The coarse powder was extracted using methanol in Soxhlet's apparatus for 96 hours, not exceeding 40°C. The extract was condensed to a semi-solid in a rotary evaporator at lowered pressure.

GC-MS analysis: Shimadzu QP2010 system (Shimadzu, Milan, Italy) with an AOC-20 auto-injector was used for Gas Chromatography-Mass Spectrometry (GC-MS) analysis. The Solution software suite was used to collect and process the data. To separate the components, a Supelco Wax column (Merck, Darmstadt, Germany) was used. With minor adjustments, the chromatographic conditions were modified from a previously published procedure[20]. The objective of the investigation was to qualitatively identify the different bioactive components that were present in the extract.

### 2.2.1 Molecular Docking and ADMET Analysis[21-23]

i. Protein preparation and receptor grid generation: Using normal procedures, the protein data bank was consulted to get the crystal structure of human serum albumin complexed with diclofenac (PDB ID: 6MA7). This structure was then ready for docking.
ii. Ligand preparation: The LigPrep module was used to process the ligands, utilising the OPLS_5 force field to minimise energy and optimise molecular geometry.
iii. Molecular docking: To assess binding positions and interaction affinities, ligand docking was carried out using the GLIDE docking module.
iv. Binding free energy calculation: The relative binding free energies of the docked ligands were estimated using the Prime/MM-GBSA method, which shed light on their binding stability and possible effectiveness.

#### 2.2.1.1 Application of QbD

By using CCD, it lists a few chosen factors. The investigation was conducted using the Design Expert software 12.0.1.0. Formula 2-2 was used for the study's independent and dependent variables over nine experimental runs. PDI and % entrapment efficiency are the dependent variables, while Lecithin (X1) and ethanol (X2) are the independent variables. An ANOVA-significant model summarises the current investigation.

### 2.2.2 Preparation of Nanoethosomes

A simple cold approach was used to create nanoethosomes. In a nutshell, lecithin (100–300 mg) was continuously stirred by magnetic stirring at 30°C in a hermetically sealed flask containing an ethanol solution (7.5-21 % v/v). Then, using a syringe, a fine stream of 5% *J. curcas* (JC) seed extract was administered gradually. The extract had previously been dissolved in ethanol. Distilled water was used to modify the final volume. To minimise vesicle size and even dispersion, the resultant mixture was probe sonicated for 30 minutes after being swirled for 15 minutes at 800–900 rpm. After being loaded with JC seed extract, the generated nanoethosomes were kept at room temperature until they were needed again. Table 1 lists the nine formulations (JCE1–JCE9) that were created using different ethanol and lecithin concentrations.

### 2.2.3 Preparation of Ethosomal Gel[24-28]

Ethosomal vesicle suspensions were incorporated by the dispersion method using Carbopol 934 as a dispersing gelling agent. The specified amount of Carbopol 934 powder was allowed to swell overnight. Tri-ethanolamine was added drop by drop to the neutralised mixture, and optimised ethosomal dispersion was added and mixed properly. A suitable

**Table 1.** Application of Central Composite Design (CCD) for the optimisation of the formulation

| Code | Lecithin (mg) | Ethanol (v/v) | PDI (nm) | Entrapment Efficiency (%) |
|---|---|---|---|---|
| JCE-1 | 100 | 7.5 | 0.807 | 48.3 |
| JCE-2 | 300 | 7.5 | 0.923 | 50.4 |
| JCE-3 | 100 | 21 | 0.721 | 55.5 |
| JCE-4 | 200 | 21 | 0.608 | 72.9 |
| JCE-5 | 100 | 15 | 0.894 | 44.3 |
| JCE-6 | 300 | 15 | 0.898 | 55.6 |
| JCE-7 | 200 | 7.5 | 0.899 | 45.9 |
| JCE-8 | 300 | 21 | 0.368 | 81.8 |
| JCE-9 | 200 | 15 | 0.948 | 45.7 |

preservative was added after the mixture had been mixed until a clear, translucent gel had formed. After that, the produced gels were put into glass containers and kept for later analysis between 4 and 8°C.

#### 2.2.3.1 Characterisations of Ethosome Gel

##### 2.2.3.1.1 Fourier Transform Infrared Spectroscopy (FT-IR)

The functional groups of the bioactive substances found in the methanolic extract were determined by analysing the overlay spectra. The existence and encapsulation of bioactive ingredients were confirmed by the comparison of the extract's and the ethosomal formulation's spectra, which offered important insights into the distinctive functional groups, especially in the 400–4000 $cm^{-1}$ spectral region.

##### 2.2.3.1.2 Scanning Electron Microscopy (SEM)

The produced nanoethosomes' surface properties and shape were examined with a SEM (JEOL JSM-50A, Tokyo, Japan). Double-sided sticky tape was used to carefully place freeze-dried ethosome samples onto aluminium stubs, and a razor blade was used to break them apart and reveal the internal structures. A thin layer of gold/palladium was then sputter-coated onto the samples for 120 seconds at a current of 14 mA in an argon environment. To assess the surface morphology of the nanoethosomes, SEM imaging was carried out utilising secondary electron emission at an accelerating voltage of 20 kV.

##### 2.2.3.1.3 Zeta Potential and Particle Size Distribution

Using a Zetasizer Nano (Malvern Instruments, UK), Dynamic Light Scattering (DLS) analysis was carried out to ascertain the ethosomal formulations' zeta potential and particle size distribution at 25°C. The formulation with the smallest particle size and an acceptable zeta potential was chosen for additional characterisation and assessment out of all the created batches.

##### 2.2.3.1.4 Entrapment Efficiency

A chilled centrifuge was used to centrifuge 100 mg aliquots of the optimised JCE gel for 30 minutes at 1100 rpm. The ethosomal pellet was carefully removed from the clear supernatant. A vacuum oven was then used to dry the pellet. To guarantee full lysis of the ethosomes, a precisely weighed 25 mg piece of the dry pellet was dissolved in 10 mL of methanol and sonicated for 20 to 30 minutes. PBS, or phosphate-buffered saline, was used to further dilute the resultant solution (pH 7.4). Both the reconstituted pellet solution and the supernatant had their absorbance measured at λmax 279 nm. The following formula was used to compute the % entrapment efficiency after the total drug content in the dispersion was established.

% Entrapment efficiency = amount of *J. curcus* gel in sediment/amount of added X 100.

## 2.3 Stability Studies

In order to conduct stability tests, the optimised ethosome gel was kept in lacquered aluminium collapsible tubes at three distinct temperatures for three months: 4 ± 2 °C, 25 ± 2 °C, and 40 ± 2 °C. Following the previously outlined analytical procedures, the formulations were assessed for changes in drug content, viscosity, pH, colour, and physical appearance at predefined intervals[29].

## 2.3 *In Vitro* Drug Release Study

A Franz diffusion cell with a dialysis membrane was used to perform the formulation's *in vitro* diffusion research. The dialysis membrane was pre-soaked in distilled water for a full day before usage. An upper donor compartment and a lower receptor compartment made up the Franz diffusion cell. While 100 mL of the ethosomal formulation was positioned in the donor compartment across the membrane, with an effective diffusion area of 2 $cm^2$ exposed to the receptor medium, the receptor compartment was filled with phosphate buffer (pH 7.4). Using a magnetic stirrer, the complete assembly was kept at 600 rpm for a total of 10 hours. To maintain sink conditions, samples were taken out at one-hour intervals and promptly replaced with an equivalent volume of brand-new phosphate buffer. To ascertain drug release, the gathered samples were suitably diluted with buffer and subjected to spectrophotometric analysis at a wavelength of 295 nm[30,31].

Various kinetic models were used to characterise the release kinetics: zero-order, first-order, Higuchi's model, Hixson-Crowell, and Korsmeyer-Peppa's model.

## 2.4 *In Vitro* Activity

### 2.4.1 Anti-inflammatory Activity

Human Red Blood Cell (HRBC) membrane stabilisation method: Blood was collected from healthy

volunteers who had not taken Non-Steroidal Anti-Inflammatory Drugs (NSAIDs) for at least two weeks before the study. The collected blood was mixed with an equal volume of sterile Alsever's solution containing 2% dextrose, 0.8% sodium citrate, 0.05% citric acid, and 0.42% sodium chloride in water, and then centrifuged at 3000 rpm. The packed erythrocytes were washed three times with isosaline (0.85%, pH 7.4), and a 10% v/v HRBC suspension was prepared using the same solution. The assay mixture consisted of 0.5 mL of different concentrations of the extract (62.5, 125, 250, 500, and 1000 µg/mL) or the standard drug aspirin at corresponding concentrations, along with 1 mL of phosphate buffer (0.15 M, pH 7.4), 2 mL of hyposaline (0.36%), and 0.5 mL of the HRBC suspension. For the control, 2 mL of distilled water was used instead of hyposaline. All assay mixtures were incubated at 37°C for 30 minutes and subsequently centrifuged. The haemoglobin content in the supernatant was measured spectrophotometrically at 560 nm using a UV spectrophotometer. The percentage of haemolysis was calculated by considering the haemolysis produced in the presence of distilled water as 100%, and the percentage of HRBC membrane stabilisation or protection was determined using the standard formula.

Protein denaturation method: Preparation of 1% of egg albumin solution: Fresh hen's eggs or egg albumin powder that is readily accessible in stores can be used to make a 1% egg albumin solution. Making egg-albumin solution using a fresh hen's egg properly involves carefully cracking an egg, transferring 1 mL of the translucent portion to 100 mL of w/V distilled water, and stirring thoroughly. The clear component of the egg is called egg albumin. The water should be cold when making the solution. Water will coagulate if it is heated to a boil.

Standard concentration series were prepared, and they are Aspirin (62.5, 125, 250, 500, 1000µg/mol) was used as a positive control. All the concentration series were made similarly. Phosphate buffer saline (PBS, pH 6.4) was made using 28.80 g of the disodium salt of hydrogen phosphate and 11.45 g of dipotassium salt of hydrogen phosphate dissolved in 1000 mL of distilled water. For the preparation of determined test samples, 2.8 ml of PBS, 0.2 ml of egg albumin, and 0.2 ml of the extract and formulation were added. For the reference drug, Aspirin test samples were prepared using 2.8 ml of PBS, 0.2 ml egg albumin, and 0.2 ml Aspirin. A control sample was prepared using 2.8 ml of PBS, 2 ml of distilled water, and 0.2 ml of egg albumin. All prepared samples were incubated at 37°C in the water bath for 15-20 minutes using the laboratory shaking water bath, followed by heating at 70°C for five minutes. Allowed the samples to cool for 10 minutes at room temperature. Absorbances were taken at 660 nm against a blank, using the double-beam UV-Visible spectrophotometer. The whole test procedure was done in triplicate. % inhibition of egg albumin denaturation was measured using the following equation[32].

Percentage protection = (Optical density of control-Optical density of test) /Optical density of control X 100.

### 2.4.2 Antimicrobial Activity

Fungal growth conditions: First, pure fungal cultures were inoculated into Sabouraud Dextrose Agar (SDA) plates, which were then incubated for 24 hours at 37°C. Fresh fungal growth was aseptically placed into 2 mL of sterile 0.145 mol/L saline solution to create the inoculum. The resultant suspension's turbidity was brought into compliance with the 0.5 McFarland standard, which corresponds to a fungal concentration of roughly $1.5 \times 10^8$ CFU/mL. The testing for antifungal tolerance was then conducted using this standardised inoculum[33].

The agar well diffusion method (also known as the Kirby-Bauer technique) was used to assess the antifungal activity against *Candida albicans*. Sterile cotton swabs were used to evenly swab the fungus suspension onto SDA agar plates. A sterile cork borer was used to construct wells that were 6 mm in diameter and spaced about 2 cm apart. 100 µL of test materials at concentrations ranging from 50 to 500 µg/mL were added to each well. After allowing diffusion at ambient temperature, the plates were incubated for 48 hours at 37°C. Using a clear ruler, Zones Of Inhibition (ZOI) were measured in millimetres[34,35].

The serial dilution approach was used to find the MIC in accordance with CLSI recommendations and Eloff's methodology. The test material was serially diluted in Sabouraud Dextrose Broth in concentrations varying from 1000 to 31.25 µg/mL. A 100 µL suspension of *C. albicans* was added to each tube for inoculation. The negative (broth only) and fungal (culture only)

controls were included, while the positive control was fluconazole (150 µg/mL).

A spectrophotometer was used to detect absorbance at 600 nm after tubes were incubated for 48 hours at 28 to 35 °C. The lowest concentration that did not exhibit any discernible development (clear tube) was the MIC. Minimum Fungicidal Concentration (MFC) was defined as the sample's lowest concentration that, following 48 hours of incubation at 35°C, inhibited 99.9% of fungal growth. 10 µL from the MIC tube and the subsequent higher concentration tube were plated on SDA agar for MFC evaluation. Colonies were counted following a 48-hour incubation period at 35°C. The MFC was identified as the lowest concentration with no discernible growth. All extracts, fractions, and isolated substances underwent this test[36].

The agar well diffusion (Kirby-Bauer) method was used to evaluate the antifungal activity against *M. canis* and *M. audouinii*. Sterile cotton swabs were used to swab fungal solutions onto SDA plates. A sterile cork borer was used to produce six wells, each measuring 6 mm in diameter and about 2 cm apart. 100 µL of test samples with concentrations ranging from 125 to 1000 µg/mL were added to each well. After allowing for diffusion at ambient temperature, the plates were incubated for 48 hours at 37°C. A clear ruler was used to measure the zones of inhibition in millimeters[37,38].

No antifungal action was thought to be indicated by the lack of a zone of inhibition[39,40]. Based on the diameter of the inhibitory zone, activity was categorised as sensitive (>11 mm), moderate (8–10 mm), and resistant (<7 mm)[41]. In this investigation, fluconazole (150 µg/mL) served as the standard control.

### 2.5 Statistical Analysis

Data were expressed as mean ± standard error of mean and analysed using independent t-tests with SPSS 17.0. Significance was considered at $p < 0.05$. Graphs were prepared using GraphPad Prism 8.

## 3. Results

### 3.1 GC-MS Analysis

A total of five compounds were identified in the methanolic seed extract. 9,12-Octadecadienoic Acid (Z, Z)- is present in the highest concentration, which is 69.7%.

### 3.2 Molecular Docking and ADMET Analysis

Together with the reference compound Fluconazole, Table 2 summarises the docking score, ΔG binding energy values, 2D and 3D interaction images, hydrogen bond interactions with amino acid residues, and bond distances of the compounds that were identified from the seed extract with the target protein (PDB ID: 6MA7). The chemical structures and 2D and 3D interaction images of Fluconazole are shown in Figure 1.

9,12-Octadecadienoic acid (Z,Z) showed the binding energy (-79.46 kcal/mol) and the highest positive docking score (-7.272) among the phytoconstituents that were found, indicating a strong binding affinity. In the extract, this chemical was also present in the largest amount. Other compounds showing significant interactions include n-Hexadecanoic acid (docking score: -6.161; ΔG: -76.89 kcal/mol), 1,2,3,4-Tetrahydrobenzo\[a]fluorene (-5.232; -47.34 kcal/mol), (Z)6, (Z)9-Pentadecadien-1-ol (-2.703; -55.91 kcal/mol), and Z, Z-2,15-Octadecadien-1-ol acetate (-0.563; -77.97 kcal/mol).

The reference compound, Fluconazole, showed a docking score of -6.512 and a binding energy of -51.53 kcal/mol. The antimicrobial activity observed in the extract can be attributed to the synergistic or individual effects of these bioactive compounds, with 9,12-Octadecadienoic acid

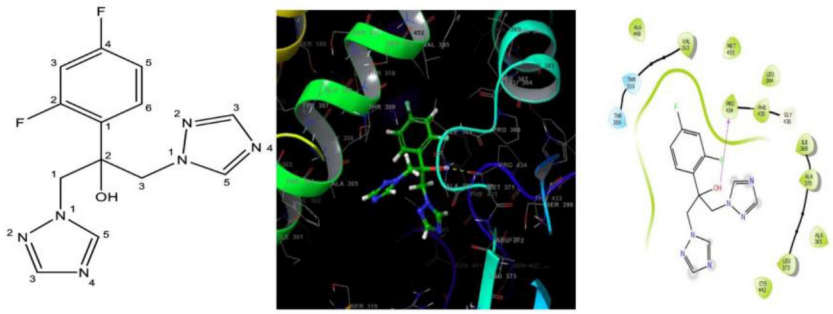
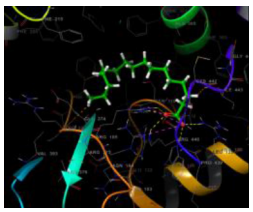
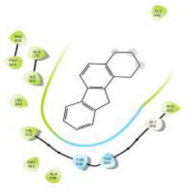
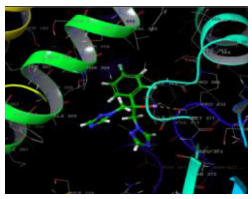
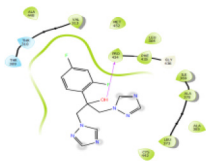
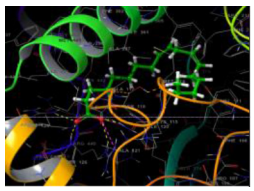
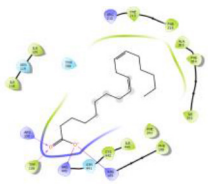
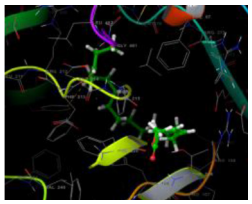
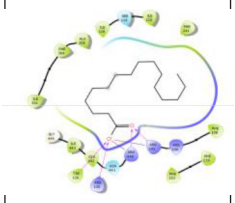
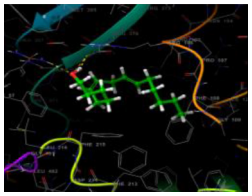
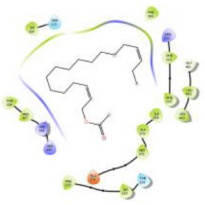
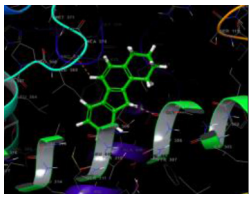
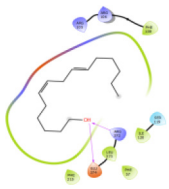



**Figure 1.** Fluconazole chemical structure, 2D and 3D images.

**Table 2.** Molecular docking and hydrogen bond studies of the *J. curcus* seed extract with PDB ID: 6MA7

| Compound Name | Dock Score | MM GBSA dG Bind | 3D Image | 2D Image | 2D Interaction | Distance ($A^0$) |
|---|---|---|---|---|---|---|
| N-HEXADECANOIC ACID | -6.161 | -76.89 |  |  | H-BOND: ARG130, TRP126, ARG440, ARG105 SALT BRIDGE: ARG440, ARG105 | 2.10,1.74,2.46, 1.88 4.94,4.93 |
| 9,12-OCTA DECADIENOIC ACID (Z,Z)- | -7.272 | -79.46 |  |  | H-BOND: ARG130, TRP126 SALT BRIDGE: ARG440, ARG105 | 2.09,1.88 4.06,3.00 |
| Z, Z-2,15-OCTA DECEDIEN-1-OL ACETATE | -0.563 | -77.97 |  |  | NO INTERACTION | NO DISTANCE |
| (Z)6,(Z)9-PENTA DECADIEN-1-OL | -2.703 | -55.91 |  |  | H-BOND: ARG372, GLU374 | 2.07,1.65 |
| 1,2,3,4-TETRA HYDROBENZO[A] FLUORENE | -5.232 | -47.34 |  |  | NO INTERACTION | NO DISTANCE |
| REFERENCE FLUCONAZOLE | -6.512 | -51.53 |  |  | H-BOND:PRO434 | 1.97 |

(Z, Z) playing a predominant role. Table 2, for additional interaction parameters. The extract's pharmacokinetic properties were studied, and the results were favorable. 2D interaction and hydrogen bond distance of two bioactive molecules are, for 9,12-Octadecadienoic acid (Z, Z)- (ARG130, TRP126, Salt Bridge: ARG440, ARG105), two molecules have no interaction: Z, Z-2,15-Octadecadien-1-Ol acetate and 1,2,3,4-Tetrahydrobenzo[A]Fluorene. Out of the five compounds, three molecules were collectively responsible for biological activity against the selected target.

## 3.3 Preparation of Ethosome Gel

### *3.3.1 Application of QbD*

Thirteen formulations in all have been developed for optimisation using a Central Composite Design (CCD)

method with two independent and two dependent parameters. The software included four of these formulations as replicates in the design because they had the same values. Based on favourable Polydispersity Index (PDI) values and superior entrapment efficiency, the best formulation (JCE-8) was selected from the remaining nine distinct formulations Table 1.

#### 3.3.1.1 Response 1

PDI: There is only a 0.01% chance that the model's high F-value of 65.91 might be the result of random noise, indicating that the model is statistically significant. P-values below 0.0500 indicate the significance of the associated model terms. The quadratic terms $A^2$ and $B^2$, the interaction term AB, and factors A and B are all significant in this instance. If model terms that have p-values higher than 0.1000 are not necessary to preserve model hierarchy, it may improve the model's performance. Since the difference is less than 0.2, the adjusted $R^2$ of 0.9643 and the projected $R^2$ value of 0.7900 are in good agreement. The signal-to-noise ratio, or Adequate Precision, has a value of 24.434, which is significantly higher than the ideal cutoff of 4, suggesting a strong signal. As a result, this model can be used to navigate and optimise the design space depicted in Table 3. In Figure 2, the contour plot, 3D surfaces and predicted *vs.* actual of the best formulation have been given.

#### 3.3.1.2 Response 2

%EE: There is only a 0.01% chance that the model's high F-value of 55.67 might be the result of random noise, indicating that the model is statistically significant. Statistically significant model terms are shown by p-values below 0.0500. The quadratic term $B^2$, the interaction term AB, and factors A and B are significant in this instance. Model terms with p-values higher than 0.1000 are deemed inconsequential; their elimination may improve model performance if they are present in substantial quantities (apart from those necessary to preserve model hierarchy). Since the difference is less than 0.2, the adjusted $R^2$ of 0.9579 and the projected $R^2$ of 0.7987 are in good agreement Table 3. In Figure 2, the contour plot, 3D surfaces and predicted *vs.* actual of the best formulation have been given.

**Table 3.** ANOVA model and Fit Statistic Values for PDI and % EE

| Response | Model | F-value | p-value | $R^2$ | Adjusted $^R2$ | Predicted $R^2$ | Adeq. Precision | Std. Dev | Mean |
|---|---|---|---|---|---|---|---|---|---|
| PDI | Quadratic model-Significant | 65.91 | < 0.0001 | 0.9792 | 0.9643 | 0.7900 | 24.4337 | 0.0330 | 0.8352 |
| % EE | Quadratic model Significant | 55.67 | < 0.0001 | 0.9755 | 0.9579 | 0.7987 | 25.5395 | 2.41 | 52.55 |

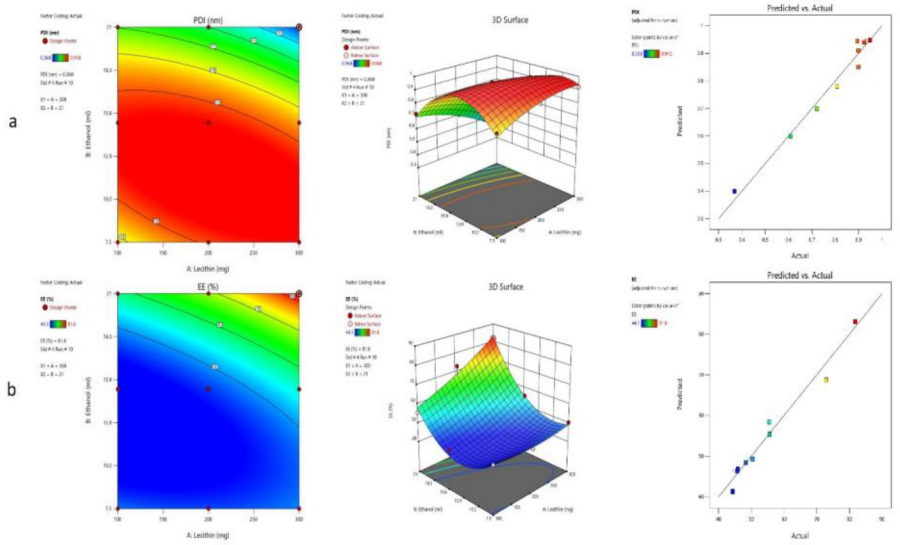



**Figure 2.** CCD inbuilt images of optimised formulation (JCE8) for (a) PDI: Contour plot, 3D and Predicted *vs.* Actual, and (b) %EE: Contour plot, 3D and Predicted *vs.* Actual.

### 3.3.2 Preparation of Ethosomal Gel

The optimised formulation JCE-8 has been further converted to a gel for enhancing the therapeutic effects.

### 3.3.3 Characterisations of Ethosome Gel

#### 3.3.3.1 FT-IR Analysis

The spectrum interpretation of the herbal ethosomal gel formulation and the pure methanolic extract. The principal peaks seen in both spectra were quite comparable, suggesting that the extract's fundamental functional groups did not alter during formulation. O-H stretching vibrations are represented by a large peak seen between 2800 and 3400 $cm^{-1}$, which implies the extract contains alcoholic chemicals. There appears to be no substantial chemical interaction between the extract and the excipients in the ethosomal system, based on the similarity of this peak in the two spectra. While distinctive absorption bands between 600 and 800 $cm^{-1}$ reveal the existence of aromatic rings, most likely because of benzene structures in the phytoconstituents, peaks in the range of 1400–1800 $cm^{-1}$ indicate the presence of alkenes.

#### 3.3.3.2 Scanning Electron Microscopy

In Figure 3, SEM was used to analyse the herbal ethosomal gel formulation's surface appearance. The SEM pictures showed that the extract was evenly distributed throughout the gel matrix, with the ethosomal vesicles typically having smooth surfaces and spherical to oval shapes. With minimal aggregation and a well-formed, distinct appearance, the vesicles suggested that the formulation was stable. Additionally, the smooth surface shape suggests that the herbal extract is effectively encapsulated within the ethosomal bilayers. The lack of crystalline structures also suggests that the active ingredients were highly integrated into the vesicular system, most likely in a form that was amorphous or molecularly distributed. These findings lend credence to the effective creation of a stable, uniform herbal ethosomal gel that may be used topically.

#### 3.3.3.3 Particle Size Distribution and Zeta Potentials

The herbal ethosomal gel formulation's particle size measurement showed that the mean vesicle size was within the nanometric range, suggesting that the ethosomal vesicles were effectively formed into nanosized particles that could be applied topically. Figure 4, where particle size showed 154.1 nm with a PDI value of 0.366. A low PDI, which indicates a restricted particle size distribution, shows that the vesicles in the formulation are stable and homogenous.

Good electrostatic repulsion between the vesicles was indicated by the zeta potential test, which had a noticeably negative result. Because it inhibits aggregation over time, this high negative zeta potential helps maintain the ethosomal system's physical stability. In Figure 4 zeta potential of the gel is indicated as -29.6 mV. The ethosomal gel formulation is stable,

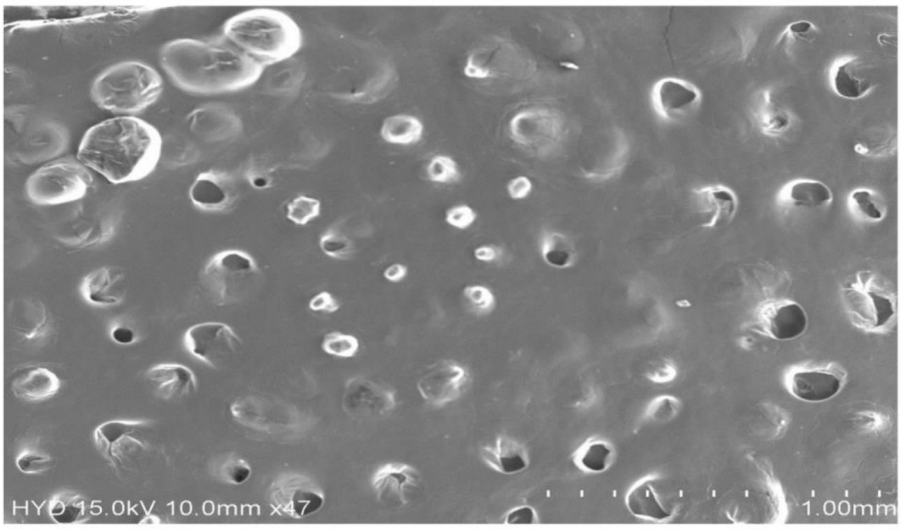



**Figure 3.** Morphology of ethosome gel (JCE8) by SEM.

well-dispersed, and appropriate for improved skin penetration and prolonged drug release, as confirmed by the combination of tiny particle size, low PDI, and high zeta potential.

### 3.3.3.4 *Entrapment Efficiency*

Efficient encapsulation of the bioactive components into the ethosomal vesicles was indicated by the substantially high entrapment efficiency of the herbal ethosomal gel formulation. The lipophilic nature of the extract's constituents and ethosomes' vesicular shape, which improve drug loading, are probably the causes of this high entrapment. The formulation's increased stability, prolonged release, and therapeutic efficacy are all guaranteed by the effective encapsulation. According to these results, ethosomal gel is a viable carrier technology for the topical administration of herbal active ingredients. In Figure 5, a study of drug release for all nine ethosome gel formulations is shown, with the highest 97% drug release from JCE 8. In Figure 6, a comparative percentage drug release of optimised nanosuspension and ethosome gel (97%) and extract (66%) have presented.

### 3.3.5 *Stability and Drug Kinetic Studies*

Stability studies: Throughout the course of the investigation, the herbal ethosomal gel formulation demonstrated exceptional chemical and physical stability in a range of storage settings. Colour, consistency, pH, and entrapment efficiency did not significantly change, suggesting the formulation's durability and long-term applicability, as shown in Table 4. The bioactive chemicals are preserved, and the therapeutic efficacy is maintained over the course of the shelf life thanks to the stability of the vesicular system.

Drug kinetic studies: A sustained release profile from the ethosomal gel was found by drug release kinetics, suggesting that the active chemicals diffused under control. A diffusion-controlled mechanism is suggested by the release data's best match to the e.g., Hixson Crowel or Higuchi model show in Figure 7. In addition to lowering dosage frequency and lengthening

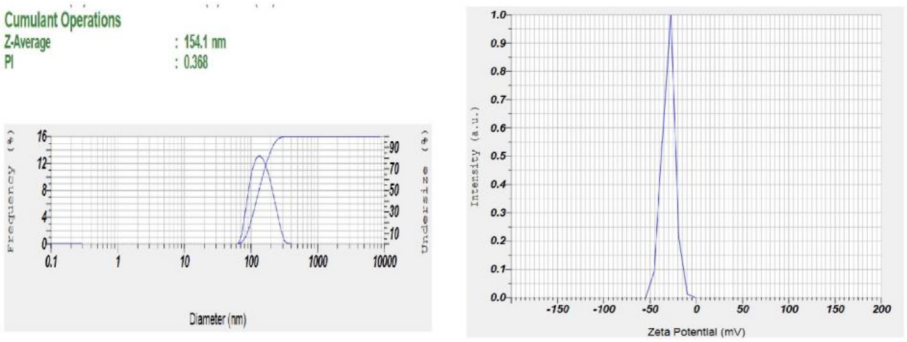



**Figure 4.** (a) Particle Size and (b) Zeta potential of ethosome gel (JCE8).

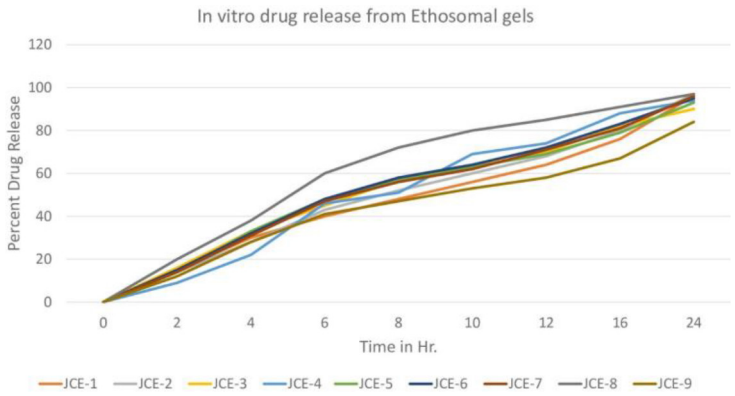



**Figure 5.** Percentage Drug release (a) Nine formulations of ethosome nanosuspension (JCE1-JCE9).

skin retention duration, this prolonged release pattern may also increase patient compliance and therapeutic results.

## 3.4 *In Vitro* Activity

### 3.4.1 Anti-inflammatory Activity

The *in vitro* anti-inflammatory activity of the extract and ethosomal formulation was evaluated using the HRBC membrane stabilisation method and the protein denaturation method. In the HRBC membrane stabilisation assay, the ability of the test samples to protect erythrocyte membranes against hypotonicity-induced lysis was assessed as an indicator of anti-inflammatory potential. The results demonstrated a clear dose-dependent increase in membrane stabilisation for all samples. Aspirin, used as the standard, showed maximum protection of 79.86% at 1000 µg/mL. The crude extract exhibited 61.96% protection, while the ethosomal formulation showed

**Table 4.** Stability data of JCE 8 Gel formulation

| Formulation | pH | Viscosity | Spreadability | Grittiness |
|---|---|---|---|---|
| JCE 1 | 7.1 | 39761 | 40.09 | NO |
| JCE 2 | 7.2 | 41872 | 39.92 | |
| JCE 3 | 7.0 | 37982 | 38.69 | |
| JCE 4 | 7.1 | 40293 | 40.93 | |
| JCE 5 | 7.0 | 42981 | 43.96 | |
| JCE 6 | 6.9 | 40163 | 42.95 | |
| JCE 7 | 7.1 | 39137 | 40.16 | |
| JCE 8 | 6.9 | 41661 | 40.87 | |
| JCE 9 | 7.3 | 40872 | 41.65 | |

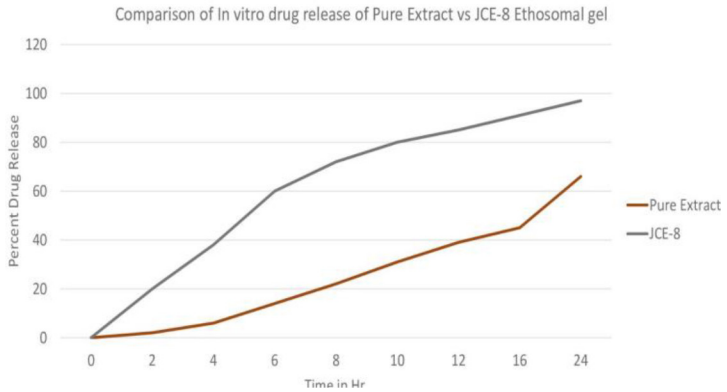



**Figure 6.** Drug release comparison of extract and gel (JCE 8).

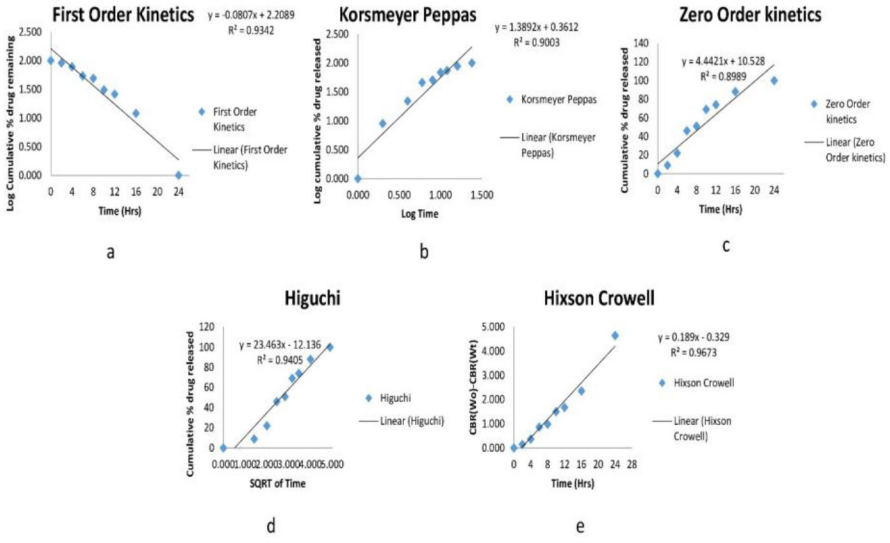



**Figure 7.** Different kinetic models of drug release in different kinetics models (a) First-order kinetics, (b) Korsmeyer Peppas, (c) Zero Order kinetics, (d) Higuchi, and (e) Hixson.

improved activity with 67.12% protection at the same concentration, indicating enhanced efficacy due to ethosomal encapsulation. Similarly, in the protein denaturation method, which evaluates the ability of samples to inhibit heat-induced denaturation of egg albumin, both extract and ethosomes demonstrated significant, concentration-dependent inhibition. Aspirin showed the highest inhibition of 80.76% at 1000 µg/mL. The extract produced 62.13% inhibition, whereas the ethosomal formulation achieved a higher inhibition of 67.75% at the same concentration. These findings suggest that the ethosomal delivery system enhances the anti-inflammatory potential of the extract by improving its interaction with protein targets and stabilising biological membranes. Overall, the study confirms that the ethosomal formulation exhibits superior anti-inflammatory activity compared to the crude extract, though slightly lower than the standard drug given in Tables 5 and 6.

### 3.4.2 Antimicrobial Activity

Antimicrobial activity of the given test compounds, viz., ME-JC with various concentrations, was assessed by the agar well diffusion method. The observed results showed satisfactory anti-fungal effect of the molecule on concentration dependent fashion against the microbe tested, *C. albicans,* in comparison to the std control used for the study. Fluconazole with 150ug/ml concentration was used as a reference std control for the current study. The antifungal activity results are shown in methanolic extract (ME-JC) against the *C. albicans* in comparison to the positive control (Fluconazole-150 ug/ml) and the negative control (Distilled water), and found that the ME-JC showed the anti-microbial activity on concentration dependent fashion (50-500 µg/ml) after 48 hours of incubation.

The MIC test demonstrates the lowest level of antimicrobial agent that greatly inhibits growth, resulting in microbial death. In the present study, MIC values of ME-JC showed the dose dependent fashion effect and confirmed the anti-fungal activity on *C. albicans.* In the present study, MIC and MBC values of ME-JC showed the dose dependent fashion inhibitory effect at 125 ug/ml and 250 ug/ml and confirmed the anti-fungal activity against the *C. albicans* sps.

Antifungal activity of the given test compound, viz., *J. curcus* ETG, with various concentrations was assessed by the agar well diffusion method. The observed results showed satisfactory anti-fungal effect

**Table 5.** HRBC membrane stabilisation method

| S. No. | Sample | % protection |
|---|---|---|
| 1 | **Control** | |
| 2 | **Standard** | 23.75 |
| 3 | | 37.17 |
| 4 | | 59.2 |
| 5 | | 70.91 |
| 6 | | 79.86 |
| | | |
| 7 | **A.O extract** | 16.18 |
| 8 | | 30.63 |
| 9 | | 41.82 |
| 10 | | 49.22 |
| 11 | | 61.96 |
| | | |
| 12 | **A.O ethosomes** | 16.86 |
| 13 | | 32.53 |
| 14 | | 47.16 |
| 15 | | 53.02 |
| 16 | | 67.12 |

**Table 6.** Protein denaturation method

| S. No. | Sample | Concentration (µg/ml) | Absorbance (660 nm) | % protection |
|---|---|---|---|---|
| 1 | **Control** | - | 0.338 | |
| 2 | **Standard** | 62.5 | 0.297 | 12.14 |
| 3 | | 125 | 0.248 | 26.62 |
| 4 | | 250 | 0.195 | 42.3 |
| 5 | | 500 | 0.121 | 64.2 |
| 6 | | 1000 | 0.065 | 80.76 |
| 7 | **Ao extract** | 62.5 | 0.302 | 12.14 |
| 8 | | 125 | 0.264 | 21.89 |
| 9 | | 250 | 0.221 | 34.61 |
| 10 | | 500 | 0.169 | 50.1 |
| 11 | | 1000 | 0.128 | 62.13 |
| 12 | **Ao ethosome** | 62.5 | 0.298 | 11.83 |
| 13 | | 125 | 0.261 | 22.98 |
| 14 | | 250 | 0.209 | 38.16 |
| 15 | | 500 | 0.146 | 56.8 |
| 16 | | 1000 | 0.109 | 67.75 |

of the molecules on concentration dependent fashion against the microbe tested, *M. audouini* (125-1000 ug/ml) *and M. canis* (125-1000 ug/ml) in comparison to the std control used for the study**.** Fluconazole with a 150 ug/ml concentration was used as a reference std control for the current study.

## 4. Discussion

*Jatropha curcus* methanolic seed extract has different bioactive compounds that were identified by GC-MS with methanolic solvent. Further, the GC-MS spectrum has been used for the molecular docking and ADMET analysis. By performing molecular docking with Human CYP3A4 bound to an inhibitor, fluconazole (PDB ID: 6MA7), antifungal activity has been predicted. In the seed extract 9,12-Octadecadienoic Acid (Z, Z)- is identified as the highest percentage, as well as good binding affinity predicted by an *in silico* study. In earlier research, the antibacterial activity of this molecule has been reported[41]. n-hexadecanoic acid isolated from *Canthium parviflorum* leaves, and its antibacterial activity has been reported. (Z)6, (Z)9-Pentadecadien-1-O, antifungal activity showed[42,43]. In the seed extract, five molecules, three of which have shown predicted antimicrobial activity, were validated by an *in vitro* study.

Quality by Design (QbD) provides several benefits for formulation development. QbD guarantees a methodical approach to comprehending the crucial formulation and process factors that affect the nanosuspension's quality[44,45].

Kerion is a severe inflammatory form of tinea capitis resulting from an exaggerated immune response to dermatophyte infection. Hence, along with antifungal therapy, control of inflammation is crucial to reduce tissue damage and scarring. In the present study, the extract and its ethosomal formulation demonstrated significant *in vitro* anti-inflammatory activity, as evidenced by HRBC membrane stabilisation and inhibition of protein denaturation in a dose-dependent manner. The ethosomal formulation showed superior anti-inflammatory efficacy compared to the crude extract, indicating enhanced bioavailability of bioactive constituents. This membrane-stabilising and protein-protective effect suggests effective suppression of inflammatory mediators. Therefore, the promising anti-inflammatory activity of the ethosomal formulation may be beneficial in reducing the inflammatory severity of kerion, supporting its potential role as an adjunct therapeutic approach in inflammatory dermatophytic infections.

There are numerous significant benefits to using Central Composite Design (CCD) to optimise seed extract nanosuspension. With fewer experimental runs, CCD, a component of Response Surface Methodology (RSM), allows for the effective evaluation of numerous formulation and process variables. It assists in determining how important variables like stabiliser concentration, sonication duration, and homogenization speed affect responses like particle size, polydispersity index, and zeta potential both singly and in combination. In order to identify ideal conditions, CCD also makes it easier to create contour plots and forecast mathematical models. This statistical method decreases resource usage, lowers variability, and improves formulation robustness. All things considered, CCD encourages a more methodical, economical, and scientifically based formulation development approach[46,47].

The capacity of herbal ethosome gel to improve the efficacy and distribution of phytoconstituents through the skin makes it significant for topical use. Deeper penetration of herbal actives is made possible by alcohol-containing ethosomes, which are soft, flexible lipid vesicles that increase the stratum corneum's permeability. They offer controlled release of the active ingredients, extended skin retention, and simplicity of application when combined with a gel basis. For the treatment of skin conditions such as infections, inflammation, and wounds, this approach provides increased therapeutic efficacy, decreased systemic adverse effects, and greater bioavailability. Furthermore, the formulation is safer, biocompatible, and appropriate for long-term use in dermatological applications due to the use of natural herbal extracts[48,49].

## 5. Conclusion

Nanosuspension-based gel formulation using *J. curcus* seed extract for topical antifungal therapy. The GC-MS analysis identified bioactive compounds with therapeutic promise, which was corroborated by molecular docking and ADMET experiments that confirmed drug-likeness

and binding affinities. The formulation was improved by Central Composite Design (CCD) to attain the appropriate particle size, zeta potential, and entrapment efficiency. The incorporation into a gel matrix preserved stability and compatibility. *In vitro* drug release and kinetic experiments revealed longer and more effective release than simple extract. The formulation demonstrated strong antifungal activity against Candida albicans, *M. canis,* and *M. audouinii,* indicating its potential as an efficient topical antifungal medication.

## 6. References


1. Rahu MI, Naqvi SHA, Memon NH, Idrees M, Kandhro F, Pathan NL, Sarker MNI, Aqeel Bhutto M. Determination of antimicrobial and phytochemical compounds of *Jatropha curcas* plant. Saudi J Biol Sci. 2021; 28(5):2867-2876. https://doi.org/10.1016/j.sjbs.2021.02.019
2. Mazumdar P, Singh P, Babu S, Siva R, Harikrishna JA. An update on biological advancement of *Jatropha curcas* L.: New insight and challenges. Renew Sustain Energy Rev. 2018; 91:903-917. https://doi.org/10.1016/j.rser.2018.04.082
3. Oskoueian E, Abdullah N, Ahmad S, Saad WZ, Omar AR, Ho YW. Bioactive compounds and biological activities of *Jatropha curcas* L. kernel meal extract. Int J Mol Sci. 2011; 12(9):5955-5970. https://doi.org/10.3390/ijms12095955
4. Albino RC, Antoniassi R, de Faria-Machado AF, Ferraris FK, Amendoeira FC, Ramos DF, Silva PEA, Leitão SG, Oliveira DR. Traditional detoxification of *Jatropha curcas* L. seeds. J Ethnopharmacol. 2019; 241:111970. https://doi.org/10.1016/j.jep.2019.111970
5. He W, King AJ, Khan MA, Cuevas JA, Ramiaramanana D, Graham IA. Analysis of seed phorbol-ester and curcin content together with genetic diversity in multiple provenances of *Jatropha curcas* L. from Madagascar and Mexico. Plant Physiol Biochem. 2011; 49(10):1183-1190. https://doi.org/10.1016/j.plaphy.2011.07.006
6. Devappa RK, Makkar HP, Becker K. Localisation of antinutrients and qualitative identification of toxic components in *Jatropha curcas* seed. J Sci Food Agric. 2012; 92(7):1519-1525. https://doi.org/10.1002/jsfa.4736
7. Kamaruddin A, Harun WHAW, Bakri MM, Abidin SAZ, Giribabu N, Syed Abdul Rahman SN. Phytochemical profile and antimicrobial activity of *Jatropha curcas* extracts against oral microorganisms. Heliyon. 2024; 10(17):e33422.https://doi.org/10.1016/j.heliyon.2024.e33422
8. Sharma AK, Gangwar M, Kumar D, Nath G, Kumar Sinha AS, Tripathi YB. Phytochemical characterisation, antimicrobial activity and reducing potential of seed oil, latex, machine oil and presscake of *Jatropha curcas*. Avicenna J Phytomed. 2016; 6(4):366-375.
9. Ebuehi OA, Okorie NA. Phytochemical screening and quantification of flavonoids from leaf extract of *Jatropha curcas* Linn. Nig Q J Hosp Med. 2009; 19(4):200-205. https://doi.org/10.4314/nqjhm.v19i4.54526
10. Dada EO, Ekundayo FO, Makanjuola OO. Antibacterial activities of *Jatropha curcas* (LINN) on coliforms isolated from surface waters in Akure, Nigeria. Int J Biomed Sci. 2014; 10(1):25-30. https://doi.org/10.59566/IJBS.2014.10025
11. Abdelgadir HA, Van Staden J. Ethnobotany, ethnopharmacology and toxicity of *Jatropha curcas* L. (Euphorbiaceae): A review. S Afr J Bot. 2013; 88:204-218. https://doi.org/10.1016/j.sajb.2013.07.021
12. Ait Babahmad R, Aghraz A, Boutafda A, Papazoglou EG, Tarantilis PA, Kanakis C, Hafidi M, Ouhdouch Y, Outzourhit A, Ouhammou A. Chemical composition of essential oil of *Jatropha curcas* L. leaves and its antioxidant and antimicrobial activities. Ind Crops Prod. 2018; 121:405-410. https://doi.org/10.1016/j.indcrop.2018.05.030
13. Rampadarath S, Puchooa D, Jeewon R. *Jatropha curcas* L: Phytochemical, antimicrobial and larvicidal properties. Asian Pac J Trop Biomed. 2016; 6(10):858-865. https://doi.org/10.1016/j.apjtb.2016.01.019
14. Rahu MI, Naqvi SH, Memon NH, Idrees M, Kandhro F, Pathan NL, Sarker MNI, Bhutto MA. Determination of antimicrobial and phytochemical compounds of *Jatropha curcas* plant. Saudi J Biol Sci. 2021; 28(5):2867-2876. https://doi.org/10.1016/j.sjbs.2021.02.019
15. Guleria D, Sagar A, Sehgal AK, Rana J, Rana J. *Jatropha curcas* L.: A comprehensive study on antibacterial, antioxidant, and phytochemical properties. Proc Natl Acad Sci India Sect B Biol Sci. 2025; 95(1):25-36. https://doi.org/10.1007/s40011-024-01634-z
16. Kuta FA, Saidu AN, Aluwo HH. Antibacterial activity of the stem bark of *Jatropha curcas* L. against four bacterial species. Braz J Biol Sci. 2015; 2(3):75-78.
17. Anyanwu OO, Eze PM, Nnaoma EI, Ngwoke KG. Antimicrobial properties of *Jatropha curcas* L. against dental pathogens. Glob J Med Res. 2018; 18(2):13-18.
18. Igbinosa OO, Igbinosa IH, Chigor VN, Uzunuigbe OE, Oyedemi SO, Odjadjare EE, Okoh AI, Igbinosa EO. Polyphenolic contents and antioxidant potential of stem bark extracts from *Jatropha curcas* (Linn). Int J Mol Sci. 2011; 12(5):2958-2971. https://doi.org/10.3390/ijms12052958
19. Zengin G, Mahomoodally MF, Sinan KI, Ak G, Etienne OK, Sharmeen JB, Brunetti L, Leone S, Di Simone SC, Recinella L, Chiavaroli A, Menghini L, Orlando G, Jekő J, Cziáky Z, Ferrante C. Chemical composition and biological properties of two *Jatropha* species: Different parts and different extraction methods. Antioxidants (Basel). 2021; 10(5):792. https://doi.org/10.3390/antiox10050792
20. Kanakal MM, Abbas SA, Khan A, Sultana S, Fatima H, Tabasssum R, Ahmed MG, Sultana R, Mohammed JS, Salfi R. Using quality by design tools to study gel formulation

from *Brassica juncea* leaves and conducting its *in vitro*, *in vivo*, molecular docking, and ADMET analyses. Anti-Inflammatory Antiallergy Agents Med Chem. 2024; 23(3):187-204. https://doi.org/10.2174/0118715230309053240718122527

21. Kumar V, Varshney P, Taleuzzaman M, Jamal R, Pal AK, Fahemoddin SM, Patil PM. *In-silico* screening of kewra oil composition and validation of its anti-arthritic efficacy against an experimental rat model. Chem. Biodivers. 2025:e202403103. https://doi.org/10.1002/cbdv.202403103
22. Haque Z, Taleuzzaman M, Jamal R, Al-Qahtani NH, Haque A. Targeting protein receptors and enzymes for precision management of urolithiasis: A comprehensive review. Eur J Pharmacol. 2024; 981:176904. https://doi.org/10.1016/j.ejphar.2024.176904
23. Aati HY, Rauf A, Al-Qatani J, Ghalloo BA, Al-Tweel A, Khwery M, Rao H, Sajid-Ur-Rehman M, Khan KU. GC-MS analysis, comprehensive biological profiling, molecular docking and ADMET studies of *Ficus vasta* Forssk. n-hexane extract. Future Sci OA. 2025; 11(1):2527021. https://doi.org/10.1080/20565623.2025.2527021
24. Kalusalingam A, Khan A, Kanakal MM, Abbas SA, Long CM, B T, Tan CS, Bawazir AS, T K AR, S R. Enhanced wound healing with *Rhodiola rosea* phytosomal gel: Extraction, formulation, and *in vivo* evaluation. Curr Pharm Des. 2025. https://doi.org/10.2174/0113816128359150250211053431
25. Sangkaew W, Sianglum W, Wunnoo S, Voravuthikunchai SP, Joycharat N. Bioactive substance contents and therapeutic potential for skin inflammation of an herbal gel containing *Derris reticulata* and *Glycyrrhiza glabra*. Pharm Biol. 2024; 62(1):648-658. https://doi.org/10.1080/13880209.2024.2385456
26. Ren S, Jin J, Wu X, Han B, Zhang W, Rong F, Hou W, Shi Q, Lin H, Liu J. Effect of an herbal gel for the prevention of radiation dermatitis-related symptoms: an open-label randomised clinical trial. J Dermatolog Treat. 2025; 36(1):2489595. https://doi.org/10.1080/09546634.2025.2489595
27. Jantarat C, Sirathanarun P, Chuchue T, Konpian A, Sukkua G, Wongprasert P. *In vitro* antimicrobial activity of gel containing the herbal ball extract against Propionibacterium acnes. Sci Pharm. 2018; 86(1):8. https://doi.org/10.3390/scipharm86010008
28. Bakasatae N, Sangkaew W, Kunworarath N, Ontong JC, Phoopha S, Takahashi Yupanqui C, Voravuthikunchai SP, Joycharat N. The standardised wood extract of *Albizia myriophylla*: Its potential as an active ingredient in an anti-inflammatory herbal gel formulation. Planta Med. 2022; 88(12):964-974. https://doi.org/10.1055/a-1535-2230
29. Alam P, Shakeel F, Foudah AI, Alshehri S, Salfi R, Alqarni MH, Aljarba TM. Central Composite Design (CCD) for the optimisation of ethosomal gel formulation of *Punica granatum* extract: *In vitro* and *in vivo* evaluations. Gels. 2022; 8(8):511. https://doi.org/10.3390/gels8080511
30. Salamanca CH, Barrera-Ocampo A, Lasso JC, Camacho N, Yarce CJ. Franz diffusion cell approach for pre-formulation characterisation of ketoprofen semi-solid dosage forms. Pharmaceutics. 2018; 10(3):148. https://doi.org/10.3390/pharmaceutics10030148
31. Katakam LN, Katari NK. Development of an *in-vitro* release testing method for permethrin cream formulation using the Franz Vertical Diffusion Cell apparatus by HPLC. Talanta Open. 2021; 4:100056. https://doi.org/10.1016/j.talo.2021.100056
32. Khan ABT, Fatima H, Irfan M, Khan MM, Fatima M, Patil PR, Warke SP, Patil SS, Ahmad MG, *et al.* Central composite design tool application for optimising methanolic leaves extract of *Ceiba pentandra* L. ethosome suspension gel with *in silico*, *in vitro*, and *in vivo* anti-inflammatory effects. Curr Bioact Compd. 2025; 21:1-14. https://doi.org/10.2174/0115734072354861250526073734
33. Jain A, Jain R, Jain S, Jain A, Jain R, Jain S. Sub-culturing of bacteria, fungi and actinomycetes. In: Basic Techniques in Biochemistry, Microbiology and Molecular Biology: Principles and Techniques. 2020. p. 101-103. https://doi.org/10.1007/978-1-4939-9861-6_29
34. Berkow EL, Lockhart SR, Ostrosky-Zeichner L. Antifungal susceptibility testing: Current approaches. Clin Microbiol Rev. 2020; 33(3):e00069-19. https://doi.org/10.1128/CMR.00069-19
35. Balouiri M, Sadiki M, Ibnsouda SK. Methods for *in vitro* evaluating antimicrobial activity: A review. J Pharm Anal. 2016; 6(2):71-79. https://doi.org/10.1016/j.jpha.2015.11.005
36. Kazaz I, Karaman GC, Karakus H, Kaya S, Hosbul T. Evaluation of colistin susceptibility by four phenotypic methods compared to broth microdilution in multidrug-resistant *Klebsiella pneumoniae*. BMC Microbiol. 2025; 25(1):415. https://doi.org/10.1186/s12866-025-04121-1
37. Ebani VV, Bertelloni F, Najar B, Nardoni S, Pistelli L, Mancianti F. Antimicrobial activity of essential oils against Staphylococcus and Malassezia strains isolated from canine dermatitis. Microorganisms. 2020; 8(2):252. https://doi.org/10.3390/microorganisms8020252
38. Nassar MSM, Hazzah WA, Bakr WMK. Evaluation of antibiotic susceptibility test results: how guilty a laboratory could be? J Egypt Public Health Assoc. 2019; 94(1):4. https://doi.org/10.1186/s42506-018-0006-1
39. Ibrahim N, Kebede A. *In vitro* antibacterial activities of methanol and aqueous leaf extracts of selected medicinal plants against human pathogenic bacteria. Saudi J Biol Sci. 2020; 27(9):2261-2268. https://doi.org/10.1016/j.sjbs.2020.06.047
40. Chirumamilla P, Dharavath SB, Taduri S. GC-MS profiling and antibacterial activity of *Solanum khasianum* leaf and

root extracts. Bull Natl Res Cent. 2022; 46(1):127. https://doi.org/10.1186/s42269-022-00818-9
41. Sanam MUE, Detha AIR, Rohi NK. Detection of antibacterial activity of lactic acid bacteria, isolated from Sumba mare's milk, against *Bacillus cereus*, *Staphylococcus aureus*, and *Escherichia coli*. J Adv Vet Anim Res. 2022; 9(1):53-58. https://doi.org/10.5455/javar.2022.i568
42. Umaiyambigai D, Saravanakumar K, Raj AG. Phytochemical profile and antifungal activity of the methanol extract from the *Psydrax dicoccos* (Gaertn) teys. and binn. Rubiaceae family. Int J Pharma Phytochem Ethnomed. 2017; 7:53-56. https://doi.org/10.18052/www.scipress.com/IJPPE.7.53
43. Krishnan K, Radha F, James A, Mohan A. Isolation and characterisation of n-hexadecanoic acid from *Canthium parviflorum* leaves. 2016:614-617.
44. Ahmad NM, Mohamed AH, Hasan NA, Zainal-Abidin N, Nawahwi MZ, Azzeme AM. Effect of optimisation variable and the role of plant extract in the synthesis of nanoparticles using plant-mediated synthesis approaches. Inorg Chem Commun. 2024; 161:111839. https://doi.org/10.1016/j.inoche.2023.111839
45. Kasemiire A, Avohou HT, De Bleye C, Sacre PY, Dumont E, Hubert P, Ziemons E. Design of experiments and design space approaches in the pharmaceutical bioprocess optimisation. Eur J Pharm Biopharm. 2021; 166:144-154. https://doi.org/10.1016/j.ejpb.2021.06.004
46. Beg S, Rahman M, Kawish SM, Qadir A, Taleuzzaman M, Ilyas R, Alam K, Shukla R. Quality by Design approach for systematic development of nanoformulations. In: Nanoformulation Strategies for Cancer Treatment. Elsevier; 2021. p. 353-364. https://doi.org/10.1016/B978-0-12-821095-6.00006-9
47. Beg S, Rahman Z. Central composite designs and their applications in pharmaceutical product development. In: Design of Experiments for Pharmaceutical Product Development: Volume I: Basics and Fundamental Principles. 2021. p. 63-76. https://doi.org/10.1007/978-981-33-4717-5_6
48. Ghelich R, Jahannama MR, Abdizadeh H, Torknik FS, Vaezi MR. Central Composite Design (CCD)-Response Surface Methodology (RSM) of effective electrospinning parameters on PVP-B-Hf hybrid nanofibrous composites for synthesis of HfB2-based composite nanofibers. Composites Part B: Engineering. 2019; 166:527-541. https://doi.org/10.1016/j.compositesb.2019.01.094
49. Andleeb M, Shoaib Khan HM, Daniyal M. Development, Characterisation, and stability evaluation of topical gel loaded with ethosomes containing *Achillea millefolium* L. extract. Front Pharmacol. 2021; 12:603227. https://doi.org/10.3389/fphar.2021.603227

## Author Contribution

Mohammad Yosuf Malik Damani conceptualized the study, carried out the experimental work including extraction, formulation development, in vitro studies, and data analysis, and prepared the original draft of the manuscript. Jagdish Kakadiya supervised the research work, contributed to the design of the study, provided critical revisions, and validated the final version of the manuscript. Both authors have read and approved the published version of the manuscript.